SURFACE BASED MORPHOMETRY IN ALZHEIMER's DISEASE

by

Esma Ece Uluğ

B.S., in Biomedical Engineering, Başkent University, 2011

Submitted to the Institute of Biomedical Engineering
in partial fulfillment of the requirements
for the degree of
Master of Science
in
Biomedical Engineering

Boğaziçi University
2019

ACKNOWLEDGMENTS

First, I would like to express how indebted I am to my advisor Ahmet Ademoğlu for his support especially during our coffee table discussions enriching me both on academical and on personal life matters. I strongly believe he is the best advisor in many ways that I could have throughout this process.

Secondly, I would like to thank Dr. Lütfü Hanoğlu and to his team, for having received his full support in the inital stages of my thesis, even though he was not my official advisor.

I could not have been happier in my time at Neurosignal Analysis Laboratory without its present and past members. I want to thank Ayşe Akgün for supporting me in and outside the lab and sharing with me her viewpoints. I am grateful to Seda Dumlu for her invaluable guidance and for her sharing long working hours with me.

I thank Ayla Şatır and her family for doing their best to make me feel at home in Istanbul. I feel very grateful towards my dear friends, Zehra Keskin, Büşranur Kocaer, Amine Bayraklı and Tuğba Yapıcı as they have always supported me and we have shared a great deal of valuable moments together.

I thank to Murat Özkök for introducing me to lots of new things in life and has supported me.

There are no words that can describe my best friends Merve Dikmen and Mügenur Büyükpastırmacı. Such friends are the ones who make our lives meaningful.

I would like to thank Nermin Okumuş, who was like a guiding light for me almost all life areas.

Finally, probably none of this would have been possible without the support of my family. Despite my hesitation and errors in the beginning about my career path, they have never stopped supporting me materially and emotionally, and they have always believed in me. I appreciate all their support: My mother Hülya Uluğ, my father Vedat Uluğ and my sisters Eda and Aleyna Uluğ.

This thesis is dedicated to my precious elders H.A.R. and S.R.

ACADEMIC ETHICS AND INTEGRITY STATEMENT

I, Esma Ece Uluğ, hereby certify that I am aware of the Academic Ethics and Integrity Policy issued by the Council of Higher Education (YÖK) and I fully acknowledge all the consequences due to its violation by plagiarism or any other way.

Name :

Signature:

Date:

ABSTRACT

SURFACE BASED MORPHOMETRY IN ALZHEIMER's DISEASE

Alzheimer's disease (AD) is a neurodegenerative disorder especially affecting the elderly population which is growing worldwide. In this study, surface-based morphometry analysis was performed on anatomical MR images of patients with Alzheimer's Disease (AD) and healthy control (HC) subjects using a computational anatomy toolbox called CAT(Computational Anatomy Toolbox) on SPM (Statistical Parameter Mapping) platform. MR images were obtained from a database named *Minimal Interval Resonance Imaging in Alzheimer's Disease* (MIRIAD) consisting of 46 AD patients and 23 HC subjects. The cortical thickness measurements were performed over 34 different regions on each hemisphere defined by Desikan-Killiany anatomical atlas. The t-statistics parameters of the cortical thickness values were found to be decreased in 24 regions in AD patients compared with the HC subjects. Additionally, the linear correlation values between the MMSE scores and cortical thickness values of AD and HC individuals were estimated for each atlas region. Accordingly, 28 regions exhibited a significant correlation between MMSE(Mini Mental State Examination) scores and cortical thickness values. Significant regions that were affected by AD were observed to be as parietal, temporal, frontal, cingulate and occipital lobes as reported in previous studies.

Keywords: Alzheimer's Disease, Magnetic Resonans Imaging, Surface Based Morphometry, Cortical Thickness, Computational Anatomy Toolbox, Desikan-Killiany Atlas, Mini Mental State Examination.

ÖZET

ALZHEIMER HASTALIĞINDA YÜZEY TABANLI MORFOMETRİ

Alzheimer hastalığı, özellikle dünya çapında sayıca artan yaşlı nüfusu etkileyen nörodejeneratif bir hastalıktır. Bu çalışmada, Alzheimer hastası ve sağlıklı bireylerin anatomik manyetik rezonans (MR) görüntüleri ile, SPM (Statistical Parametric Mapping) platformunda işleyen ve Hesaplamalı Anatomi Aracı (CAT) adı verilen hesaplamalı bir anatomi aracı kullanılarak, yüzey tabanlı morfometri analizi yapıldı. MR görüntüleri, 46 Alzheimer hastası ve 23 sağlıklı kişiden oluşan MIRIAD (Minimal Interval Resonance Imaging in Alzheimer's Disease) veri tabanından elde edildi. Kortikal kalınlık hesaplamaları, Desikan-Killiany anatomik atlasınca tanımlanan her yarı küre üzerindeki 34 farklı bölgede yapıldı. Kortikal kalınlık değerlerine ilişkin t-istatistiği parametrelerinin Alzheimer hastalarında, sağlıklı kontrol deneklerine kıyasla, 24 bölgede azaldığı bulundu. Ayrıca, her atlas bölgesi için Alzheimer hastası ve sağlıklı kontrol grupların MMSE (Mini Mental State Examination) skorları ile kortikal kalınlık değerleri arasında doğrusal ilintiler hesaplandı. Buna göre 28 bölgede, MMSE skorlar ile kortikal kalınlık değerleri arasında anlamlı ilinti olduğu gösterildi. Alzheimer hastalığından etkilenen önemli bölgelerin, geçmiş çalışmalarda da belirtildiği gibi, parietal, temporal, frontal, singulat ve oksipital loblar olduğu gözlemlendi.

Anahtar Sözcükler: Alzheimer Hastalığı, Manyetik Rezonans, Yüzey Tabanlı Morfometri, Kortikal Kalınlık, Hesaplamalı Anatomi Aracı, Desikan-Killiany Atlası, Mini Mental Durum Değerlendirmesi.

TABLE OF CONTENTS

LIST OF FIGURES

LIST OF TABLES

LIST OF SYMBOLS

Y	Observed Data Y
X	Design Matrix X
β	Parameter Vector
$\mathbf{e}$	Residual Error e
$\mathbf{C}$	Contrast Vector $\mathbf{C}$

LIST OF ABBREVIATIONS

AD	Alzheimer's Disease
MR	Magnetic Resonans
MRI	Magnetic Resonans Imaging
VBM	Voxel-Based Morphometry
DBM	Deformation-Based Morphometry
SBM	Surface-Based Morphometry
SPM	Statistical Parameter Mapping
HC	Healty Controls
GM	Grey Matter
WM	White Matter
CSF	Cerebrospinal Fluid
CS	Central Surface
CAT	Computational Anatomy Toolbox
MATLAB®	Matrix Laboratory
MIRIAD	Minimal Interval Resonance Imaging in Alzheimer's Disease
MMSE	Mini Mental State Examination
T1w	T1 Weighted
MNI	Montreal Neurological Institute
NINCDS	National Institute of Neurological and Communicative Disorders and Stroke
ADRDA	Alzheimer's Disease and Related Disorders Association
DKA	Desikan-Killiany Atlas
RFT	Random Field Theory

1. INTRODUCTION

Alzheimer's disease (AD) is a neurological disorder arising from the accumulation of proteins in the brain as in the form of plaques [3]. Some of the major indications of the AD are forgetfulness, confusing with time or place, change in behaviour and mood and inability to do daily cognitive activities such as understanding visual images and spatial relationships.

Almost two-thirds of the dementia cases are AD. The population of dementia doubles every 20 years and the number of patients, which is about 50 million now, is predicted to reach to 152 million by 2050. In areas where the elderly population is rising, the rate of growth may rise up fivefold in 20 years. AD and dementia cost over one trillion dollars in worldwide. There is no present cure for AD. Many experimental drug studies are currently being performed, especially with AD patients in early stage. The reason for this is to take precautions without further cell death in the brain and attempt to slow down the course of the disease [4].

While the structural character of the AD was studied, the patients were also discovered to have some modifications in their brain anatomy as a consequence of their autopsy, in relation to their cognitive impairment. AD progression exhibits enormous variability that can be connected with many variables such as genotype, age or gender. In addition, the amount and type of data available for each patient can be significantly different in real life. The histological analyses indicate a change in the neocortex with the entorhinal cortex and the hippocampus being among the first affected brain areas [5, 6]. Clinical examination and neurological anamnesis are the major determinants for the diagnosis of AD.

Neuroimaging, specifically magnetic resonance imaging (MRI), as a non-invasive method, has been gaining wider acceptance as a diagnostic tool especially in the early phase of the AD. Structural MRI data are used in morphometric studies in dementia.

Cognitive decline correlates with cortical atrophy which can be quantified by morphological analyses of the MRI [7]. Cortical thickness decreases due to a loss in gray matter which leads to cortical atrophy. A marker for AD-related cortical atrophy is established by measuring cortical density across the entire cerebrum [8]. Disease-specific brain atlases are important to detect cortical changes in AD and deformation analysis in longitudinal datasets are used estimate it [9]. The automated morphometry-based brain tissue measurement methods can be handled in three ways: Voxel-based morphometry (VBM), deformation-based (DBM) morphometry and surface-based methods (SBM). In VBM, the concepts of gray matter density and gray matter concentration are central for the interpretation of the results. Thus far, surface based methods have been used more widely than the voxel based methods partly because of the computational burden of the latter. Moreover, cortical thickness measurements have more reliability than the VBM since different regions associated with the same volume element may sometimes belong to remote regions considering the sulcal and gyral structure of the brain. Some of the main software packages used for morphometric analysis are Statistical Parameter Mapping (SPM), BrainSuite [10], BrainVISA [11] and FreeSurfer [12].

In order to estimate the cortical thickness from magnetic resonance (MR) images, the cortex is separated into a boundary between the gray matter (GM) and the cerebrospinal fluid (CSF) and between the GM and the white matter (WM). The human cerebral cortex is a heavily folded neuronal layer with an average thickness of about 2.5 mm, ranging from 1 to 4.5 mm in separate areas of the brain [13, 12].

As a cross sectional study, we applied surface based morphometry on MR images from the Minimal Interval Resonance Imaging in AD (MIRIAD) dataset consisting of 46 AD patients and 23 Healthy Controls (HC) using the Computational Anatomy Toolbox (CAT) developed on SPM running on MATLAB® environment. In addition to the structural MRI, the subjects had their Mini Mental State Examination (MMSE) as a measure of their cognitive performance. We used the Desikan-Killiany (DKA) anatomical atlas as a basis for the parcellation of the cortical surface. We studied the cortical thickness change between the patients and the healthy control subjects in 34 different regions belonging to each hemisphere defined by the atlas. We also estimated

the correlations between the cortical thickness and the MMSE of all the subjects over the same atlas regions. It is observed that both the cortical thickness and the MMSE scores correlate with the disease especially in a more pronounced way in certain brain regions.

1.1 Thesis Outline

The thesis is organized as follows: In Chapter 2, we introduce our data, surface-based morphometry and implemetation of CAT. The results are given in Chapter 3. In Chapter 4, the discussions and conclusions with further recommendations are presented.

2. METHODOLOGY

2.1 Cortical Thickness in Alzheimer's Disease

During the progression of neuropsychiatric disorders, certain features of the human cortex, such as cortical thickness and gyrification seem to alter [14]. Cortical thickness estimation using MRI is an essential technique for the diagnosis and following the progression of the neurodegeneration in AD patients.

Advances in computational imaging techniques, make it possible to measure the atrophy across the human cortex with a fairly accurate and precise manner [15, 16]. Entorhinal cortex thickness, as assessed with the FreeSurfer, was reported to be thinner in AD compared with HC groups [17, 18] yielding a difference in cortex volume ranging from %79 to %98 [19, 20].

2.2 Surface - Based Morphometry

Surface - Based Analysis (SBA) is a commonly used technique to perform cortical surface measurements [1]. There are several tools for SBA including Computational Anatomy Toolbox (http://www.neuro.uni-jena.de/cat/), Freesurfer (http:// surfer.nmr.mgh.harvard.edu), Brain Voyager (http://brainvoyager.com), and Brain Visa (http:// brainvisa.info). The first step of the SBA is the extraction of the cortex from the structural MRI data. The inner surface of the cortex is the white surface [21], which is the boundary between the GM and the WM. The outer surface of the cortex is the pial surface [22] which resides between the GM and the CSF. The surfaces can be represented by the construction of triangular meshes in which the corners are called as vertices. Then, these surfaces can be inflated after marking the gyri and sulci areas. With these surfaces in hand, various morphometric paramaters such as surface area measurements, gyrification, curvature and cortical thickness (the distance between the

white and pial surfaces) can be performed. Explicit surface models provide subvoxel accuracy, high sensitivity and robustness under different measurement circumstances determined by field strength, scanner type and brand [8].

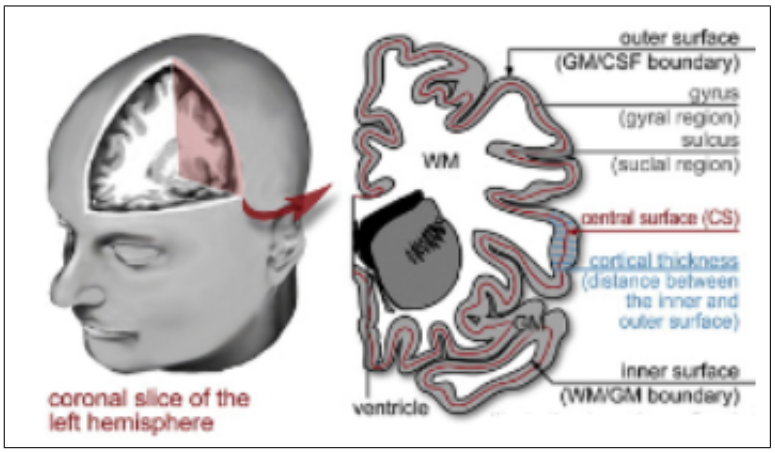

Figure 2.1 The cortex [1].

In Figure 2.1, the cortical macro-structure of the cortex is illustrated as a highly folded sheet of the GM lying inside the CSF and surrounding the WM. Inward and outwards foldings are denoted as sulci and gyri, respectively. Cortical thickness which is defined as the distance between the inner and the outer boundary is directly related to the cortical development and its degradation leads to certain diseases such as Alzheimer's.

CAT is an automatic measurement program for segmentation, quantity and thickness [9]. It is a toolbox operating on SPM and performs surface based morphometry (SBM) analysis which has several benefits over the use of voxel based methods. Surface based spatial registration is demonstrated to increase the accuracy of registration when compared with the volume-based approach. New forms of analyses, such as gyrification index which measures the surface complexity in 3D or fractal dimension, are also available in the software. Moreover, the functional activity in these regions can be visualized by inflating the sulcal regions of the cortical surface and mapping them on a sphere.

2.3 MRI Data

The MIRIAD is a database of volumetric MRI brain-scans of AD patients and healthy control people. MIRIAD data documentation is systematic and well-arranged. The anonymised scans, together with their demographic and neuropsychological data, are made available to the researchers who work on developing new techniques [23]. We employed structural T1 weighted (T1w) MR images avaliable in the MIRIAD dataset. 46 patients who were diagnosed with second grade, mild-moderate AD according to the criteria set by the NINCDS (National Institute of Neurological and Communicative Disorders and Stroke) and ADRDA (Alzheimer's Disease and Related Disorders Association) and 23 healthy subjects were used. The overview of age, gender and MMSE of the dataset is given in Tables 2.1, 2.2 and 2.3.

2.3.1 The Desikan-Killiany Atlas (DKA)

The Desikan-Killiany Atlas (DKA) is an automated, validated and reliable brain surface labeling system developed for parcelling the human cerebral cortex into standard gyral-based neuroanatomic regions [2].

As shown in Figure 2.3, the top row displays the lateral and the bottom row shows the medial views of the hemisphere. The white asterisk on the left shows the cortex around the perimeter of the central sulcus within the gyri which makes it invisible. The yellow asterisks on the right indicate the cortex around the perimeter of the "inflated" central sulcus which makes it visible.

34 cortical regions were identified in each of the hemispheres using a data set of 40 MRI scans. DKA has been used for morphometric and functional studies of the cerebral cortex in clinical trials; to monitor the evolution of disease-induced changes over time, and to examine the response to treatment [24, 25].

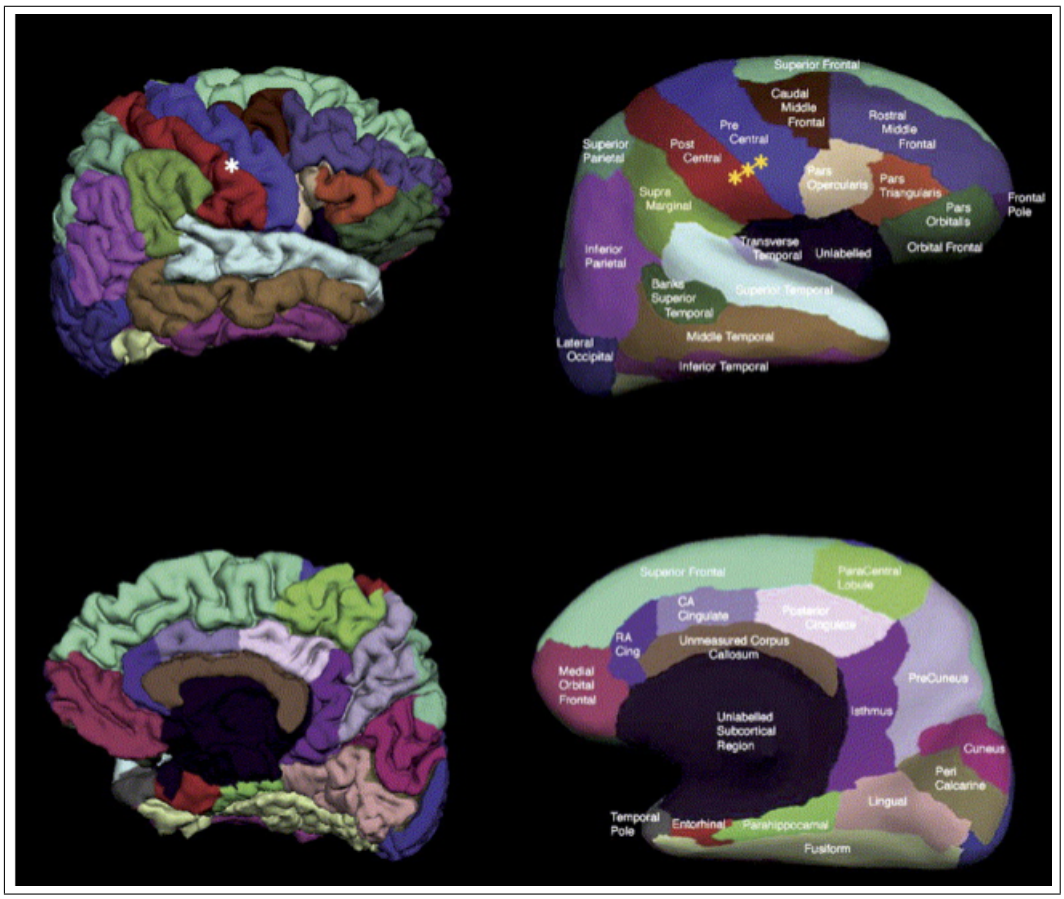

Figure 2.2 Desikan Atlas map, inflated (right) and pial (left) cortical regions in one hemisphere [2].

2.4 Surface - Based Morphometry using CAT

As a first step, the images were manually adjusted to a canonical average template using the anterior commissure with $x = 0$, $y = 0$, $z = 0$ according to the MNI (Montreal The Neurological Institute) coordinate system (Figure 2.3). Exemplar aligned HC and an AD MR images are shown in Figures 2.4 and 2.5, respectively.

After the preprocessing, the following steps were implemented in CAT;

1. Segmenting the data into three basic tissues which are the GM, WM and CSF. The boundary surfaces and the cortical thickness values are also determined for the left and right hemispheres.

2. Interpolating and smoothing the surfaces for statistical analyses. As a suggested

Table 2.1
Age Distribution Overview in MIRIAD dataset.

Age

YEARS	57 - 67	68 - 78	79 - 89
Alzheimer Group	13	26	7
Control Group	7	13	3

Table 2.2
MMSE Score Distribution Overview n MIRIAD dataset.

MMSE (Mini Mental State Examination)

SCORE	24 - 30	20 - 23	10 - 19	0 - 9
Alzheimer Group	3	9	26	8
Control Group	23	0	0	0

level of smoothing, 15 mm full-width-half-maximum isotropic Gaussian kernel is applied.

3. Statistical analysis using the General Linear Model (GLM) which is a voxel wise univariate approach in order to identify the regions that are significantly different between the patients and healthy control subjects. The GLM is expressed as

$$\mathbf{Y} = \mathbf{X}\beta + \mathbf{e} \tag{2.1}$$

where $\mathbf{Y}$ is the observed data, $\mathbf{X}$ is the design matrix encoding the covariates/confounds, β is the parameter vector and $\mathbf{e}$ is the residual error which is assumed to be zero mean. The $t-$statistics is determined as

$$t = \frac{\mathbf{C}^T\beta}{stdev(\mathbf{C}^T)\beta} \tag{2.2}$$

where $\mathbf{C} = [1 - 1]^T$ is the contrast vector showing the difference between the healthy controls and the patients. For the family-wise error control, the Random Field Theory (RFT) [26] correction is applied as a standard method in SPM. A

Table 2.3
Gender Distribution Overview in MIRIAD dataset.

Gender		
	Female	**Male**
Alzheimer Group	27	19
Control Group	11	12

statistical contrast map as a difference between the normal controls and the AD patients are shown in Figure 2.6. The details of the statistical results are given extensively in Figure 2.7.

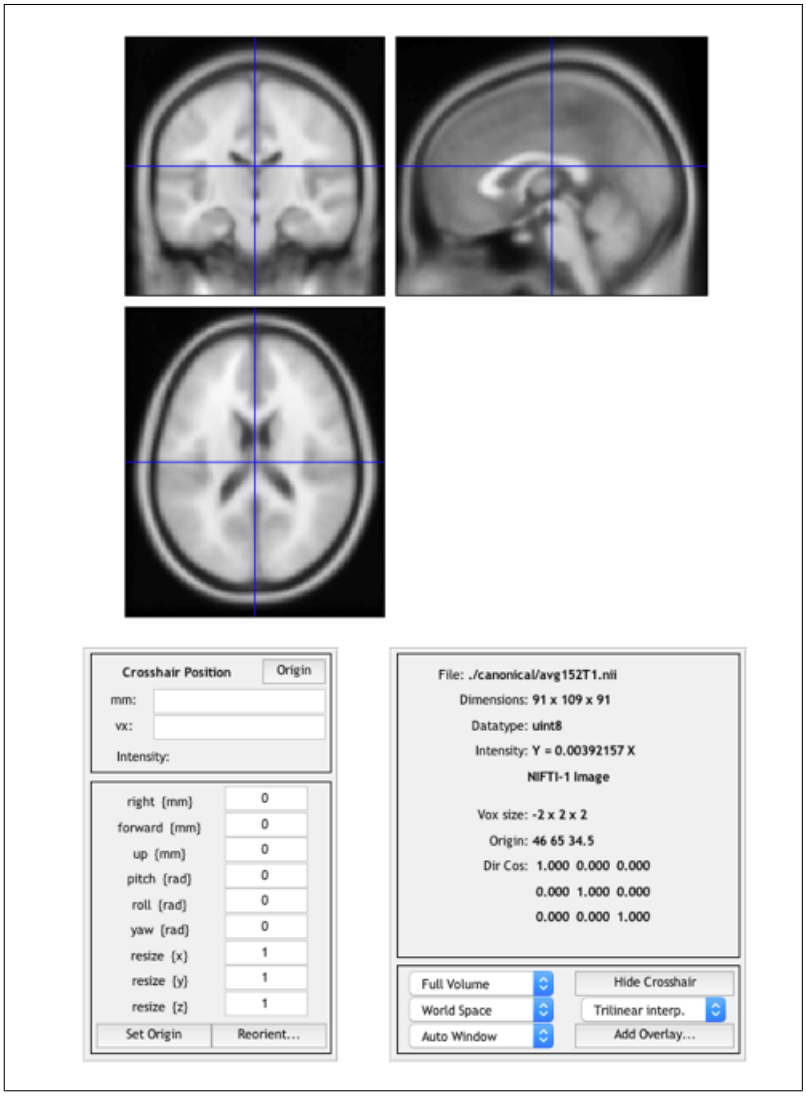

Figure 2.3 Canonical average template T1 image, in SPM package.

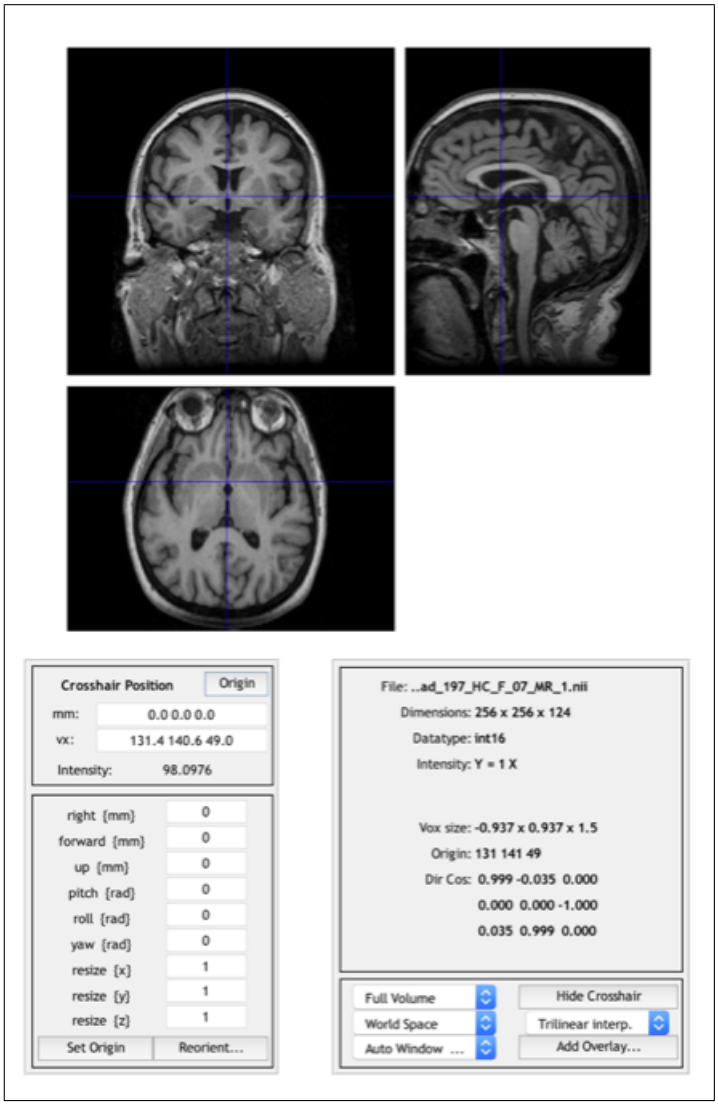

Figure 2.4 Original volumetric T1 image of a healthy control subject.

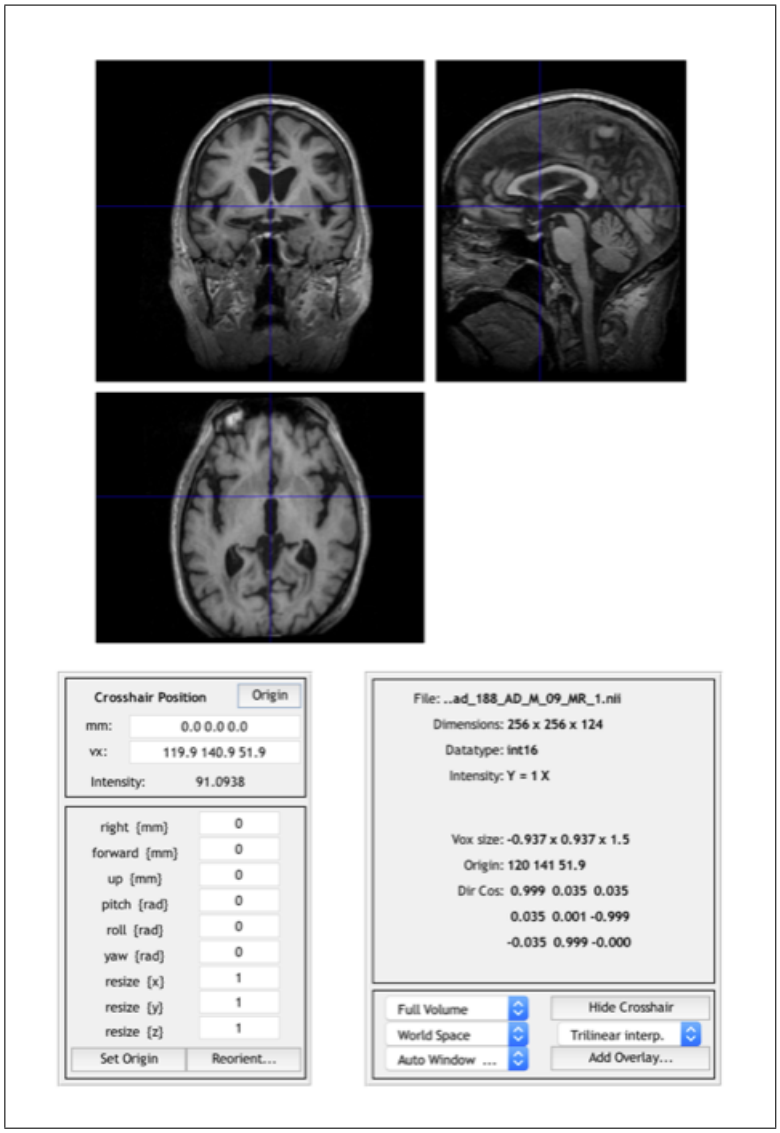

Figure 2.5 Original volumetric T1 image of Alzheimer's disease patient.

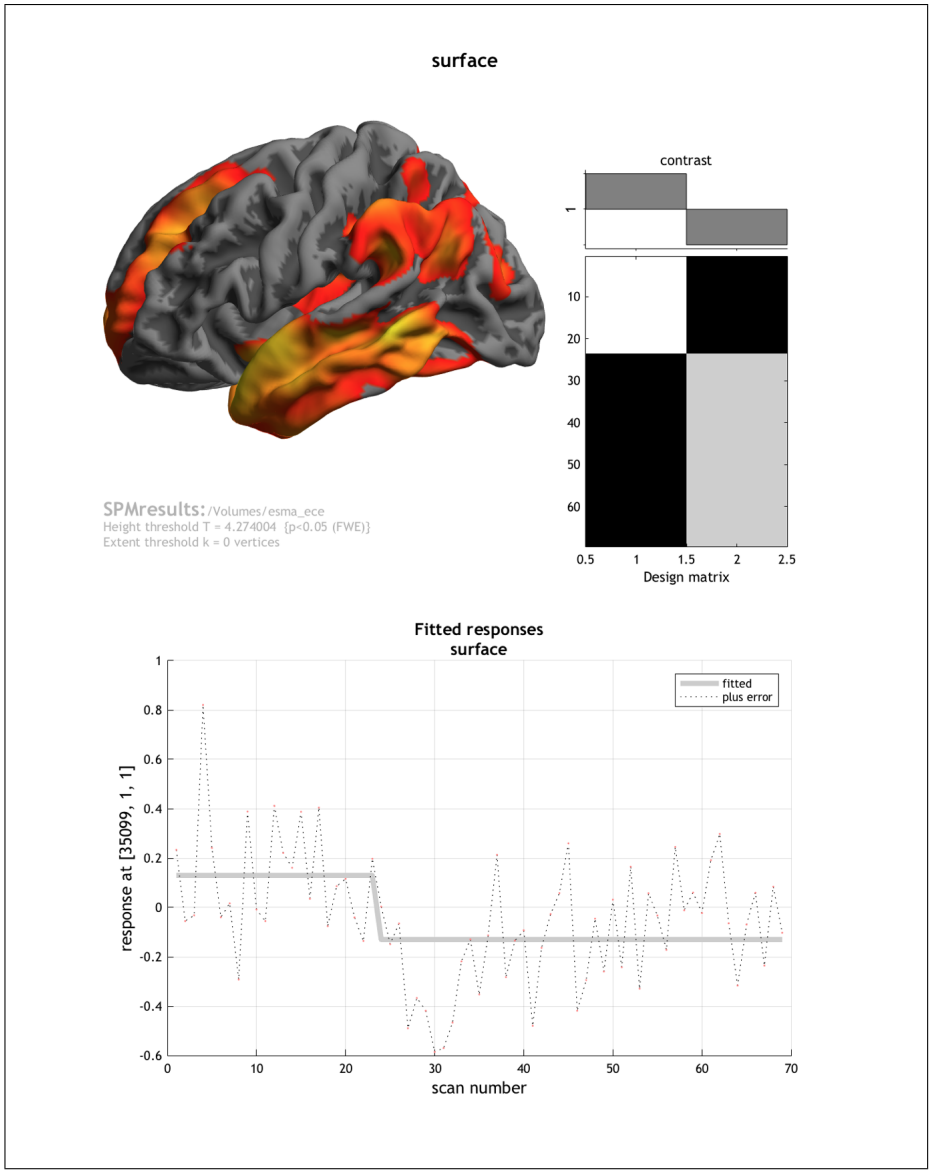

Figure 2.6 The group analysis of cortical thickness, design matrix and fitted responses.

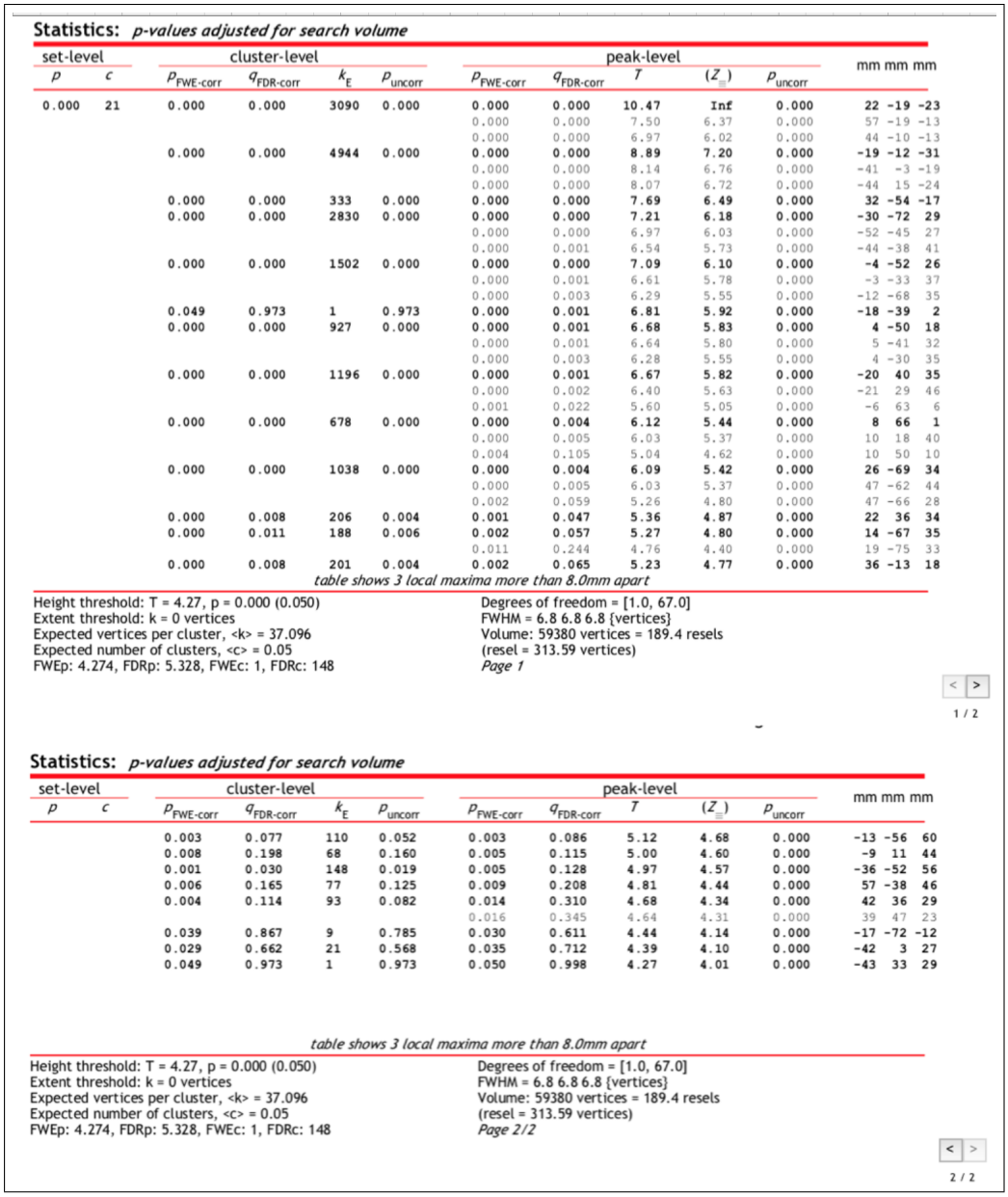

Statistics: *p-values adjusted for search volume*

set-level		cluster-level				peak-level					mm mm mm
p	c	$p_{FWE\text{-}corr}$	$q_{FDR\text{-}corr}$	k_E	p_{uncorr}	$p_{FWE\text{-}corr}$	$q_{FDR\text{-}corr}$	T	$(Z_{=})$	p_{uncorr}	
0.000	21	0.000	0.000	3090	0.000	0.000	0.000	10.47	Inf	0.000	22 -19 -23
						0.000	0.000	7.50	6.37	0.000	57 -19 -13
						0.000	0.000	6.97	6.02	0.000	44 -10 -13
		0.000	0.000	4944	0.000	0.000	0.000	8.89	7.20	0.000	-19 -12 -31
						0.000	0.000	8.14	6.76	0.000	-41 -3 -19
						0.000	0.000	8.07	6.72	0.000	-44 15 -24
		0.000	0.000	333	0.000	0.000	0.000	7.69	6.49	0.000	32 -54 -17
		0.000	0.000	2830	0.000	0.000	0.000	7.21	6.18	0.000	-30 -72 29
						0.000	0.000	6.97	6.03	0.000	-52 -45 27
						0.000	0.001	6.54	5.73	0.000	-44 -38 41
		0.000	0.000	1502	0.000	0.000	0.000	7.09	6.10	0.000	-4 -52 26
						0.000	0.001	6.61	5.78	0.000	-3 -33 37
						0.000	0.003	6.29	5.55	0.000	-12 -68 35
		0.049	0.973	1	0.973	0.000	0.001	6.81	5.92	0.000	-18 -39 2
		0.000	0.000	927	0.000	0.000	0.001	6.68	5.83	0.000	4 -50 18
						0.000	0.001	6.64	5.80	0.000	5 -41 32
						0.000	0.003	6.28	5.55	0.000	4 -30 35
		0.000	0.000	1196	0.000	0.000	0.001	6.67	5.82	0.000	-20 40 35
						0.000	0.002	6.40	5.63	0.000	-21 29 46
						0.001	0.022	5.60	5.05	0.000	-6 63 6
		0.000	0.000	678	0.000	0.000	0.004	6.12	5.44	0.000	8 66 1
						0.000	0.005	6.03	5.37	0.000	10 18 40
						0.004	0.105	5.04	4.62	0.000	10 50 10
		0.000	0.000	1038	0.000	0.000	0.004	6.09	5.42	0.000	26 -69 34
						0.000	0.005	6.03	5.37	0.000	47 -62 44
						0.002	0.059	5.26	4.80	0.000	47 -66 28
		0.000	0.008	206	0.004	0.001	0.047	5.36	4.87	0.000	22 36 34
		0.000	0.011	188	0.006	0.002	0.057	5.27	4.80	0.000	14 -67 35
						0.011	0.244	4.76	4.40	0.000	19 -75 33
		0.000	0.008	201	0.004	0.002	0.065	5.23	4.77	0.000	36 -13 18

table shows 3 local maxima more than 8.0mm apart

Height threshold: T = 4.27, p = 0.000 (0.050)
Extent threshold: k = 0 vertices
Expected vertices per cluster, <k> = 37.096
Expected number of clusters, <c> = 0.05
FWEp: 4.274, FDRp: 5.328, FWEc: 1, FDRc: 148

Degrees of freedom = [1.0, 67.0]
FWHM = 6.8 6.8 6.8 {vertices}
Volume: 59380 vertices = 189.4 resels
(resel = 313.59 vertices)
Page 1

< >
1 / 2

Statistics: *p-values adjusted for search volume*

set-level		cluster-level				peak-level					mm mm mm
p	c	$p_{FWE\text{-}corr}$	$q_{FDR\text{-}corr}$	k_E	p_{uncorr}	$p_{FWE\text{-}corr}$	$q_{FDR\text{-}corr}$	T	$(Z_{=})$	p_{uncorr}	
		0.003	0.077	110	0.052	0.003	0.086	5.12	4.68	0.000	-13 -56 60
		0.008	0.198	68	0.160	0.005	0.115	5.00	4.60	0.000	-9 11 44
		0.001	0.030	148	0.019	0.005	0.128	4.97	4.57	0.000	-36 -52 56
		0.006	0.165	77	0.125	0.009	0.208	4.81	4.44	0.000	57 -38 46
		0.004	0.114	93	0.082	0.014	0.310	4.68	4.34	0.000	42 36 29
						0.016	0.345	4.64	4.31	0.000	39 47 23
		0.039	0.867	9	0.785	0.030	0.611	4.44	4.14	0.000	-17 -72 -12
		0.029	0.662	21	0.568	0.035	0.712	4.39	4.10	0.000	-42 3 27
		0.049	0.973	1	0.973	0.050	0.998	4.27	4.01	0.000	-43 33 29

table shows 3 local maxima more than 8.0mm apart

Height threshold: T = 4.27, p = 0.000 (0.050)
Extent threshold: k = 0 vertices
Expected vertices per cluster, <k> = 37.096
Expected number of clusters, <c> = 0.05
FWEp: 4.274, FDRp: 5.328, FWEc: 1, FDRc: 148

Degrees of freedom = [1.0, 67.0]
FWHM = 6.8 6.8 6.8 {vertices}
Volume: 59380 vertices = 189.4 resels
(resel = 313.59 vertices)
Page 2/2

< >
2 / 2

Figure 2.7 Surface analysis statistic table.

3. SURFACE - BASED MORPHOMETRY ANALYSIS RESULTS

Our results reveal significant differences in cortical thickness between the two groups analyzed. The mean cortical thickness was significantly reduced in AD patients compared with the controls.

The cortical thickness measure of the superior parietal region defined in the DKA for the left and right hemispheres are shown for the AD and HC groups (Figure 3.1). As is observed, the cortical thickness difference between AD and HC groups are not the same for the same regions located at different hemisphere.

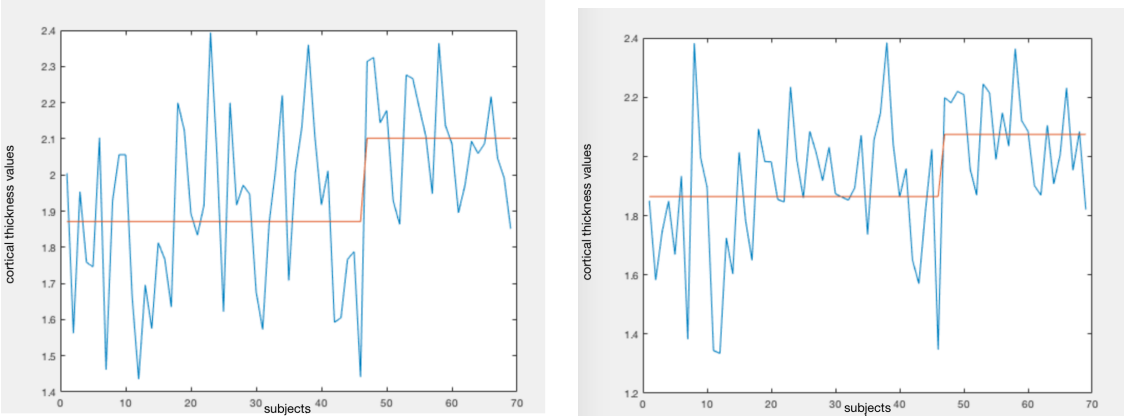

Figure 3.1 Cortical thickness values of AD patients and healthy controls in the Superior Parietal Region in the left and right hemisphere defined in DKA.

The cortical thickness measure of the post central and lateral orbito frontal regions defined in the DKA for the right and left hemisphere are shown for the AD and HC groups (Figure 3.2). The cortical thickness difference between AD and HC groups are visible for the different regions located at different hemispheres.

The statistical maps of the cortical thickness based on the contrast as a difference between the HC and AD groups (HC $>$ AD) mapped onto the DKA are shown in Figure 3.3. Six clusters are observed in the right hemisphere and three on the left. The black boundaries overlayed on the cortex are denoting the DKA atlas regions.

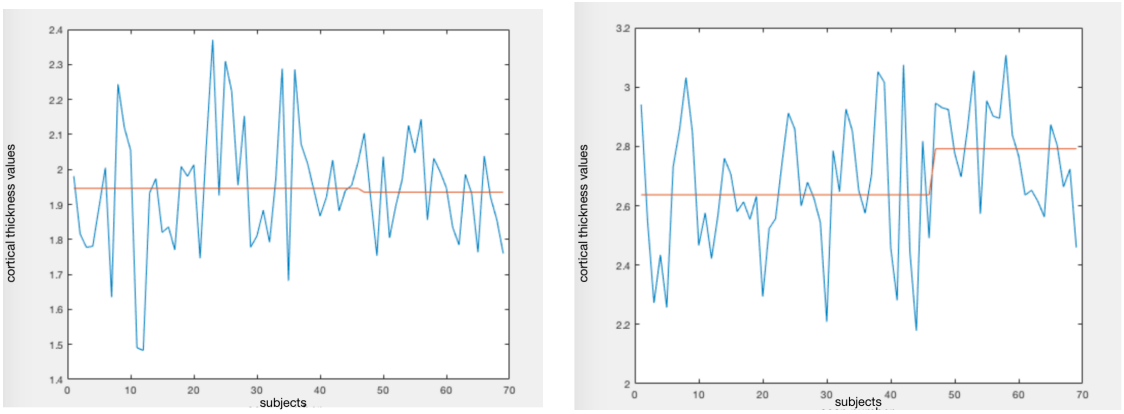

Figure 3.2 Cortical thickness values of AD patients and healthy controls in the post central (left panel) in right hemisphere and lateral orbito frontal region (right panel) in the left hemisphere.

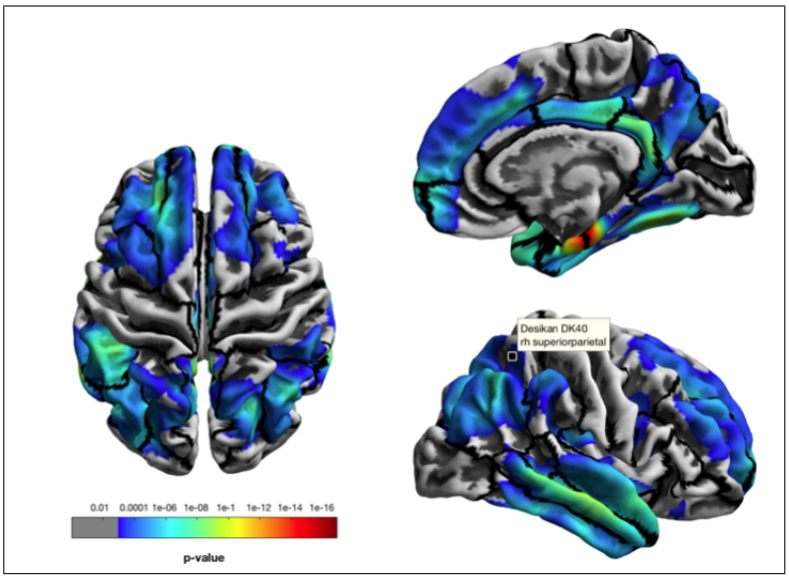

Figure 3.3 Atlas border overlay according to Desikan-Killiany Atlas.

The $t-$statistics were calculated using the cortical thickness measures from 23 HC and 46 AD subjects and tested for each anatomical region defined in DKA. The regions exhibiting a significant difference between the HC and AD group are shown in Figure 3.4 for the right and Figure 3.5 for the left hemispheres.

When the atrophy distribution is mapped on the cortical surface its regional specificity due to AD is clearly seen in Figure 3.6. The regions that show significant difference in terms of cortical thickness between the HC and AD groups are overlayed on the cortex together with their distribution on different brain regions defined by

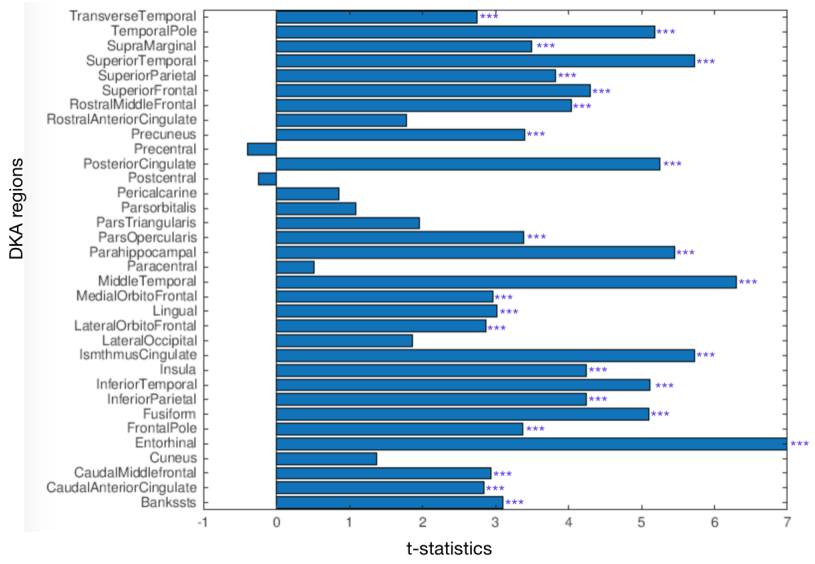

Figure 3.4 Right hemisphere $t-$statistics. Significant regions are denoted by *** ($p<0.05$).

DKA.

26 regions on the left hemisphere and 25 on the right showed significant difference in cortical thickness change between the HC and AD groups. On the other hand, 8 regions on the left and 9 regions on the right hemisphere showed no such significant change.

The relationship between the cortical thickness and MMSE scores were investigated for each anatomical region. In Figure 3.7, scatter plot of the middle temporal region for left and right hemispheres were shown. The linear correlation coefficient was estimated as 0.64 ($p<0.5$) for the right and 0.70 ($p<0.5$) for the left hemispheres. The same correlation results for each of the 34 regions in the left and in the right hemispheres are given in Figures 3.8 and 3.9.

29 regions on the left hemisphere and 28 on the right showed significant difference in cortical thickness change between the HC and AD groups. On the other hand, 5 regions on the left and 6 regions on the right hemisphere showed no such significant change.

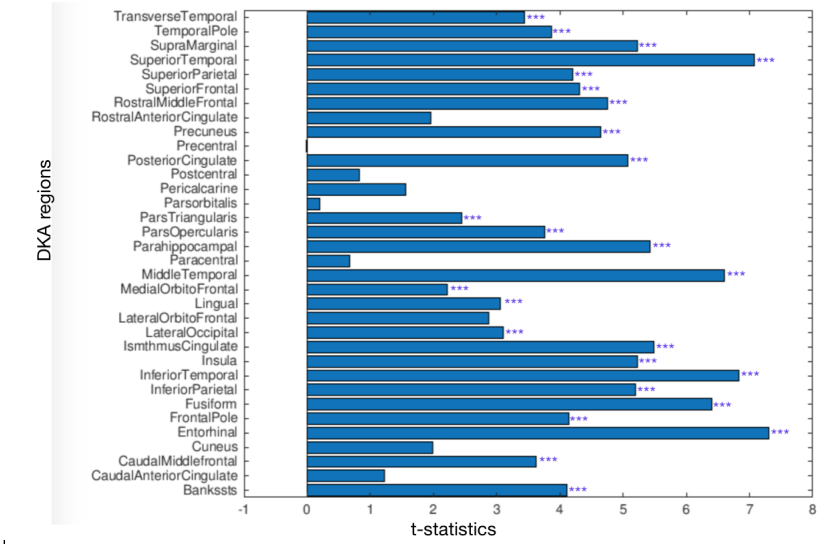

Figure 3.5 Left hemisphere $t-$statistics. Significant regions are denoted by ($p<0.05$).

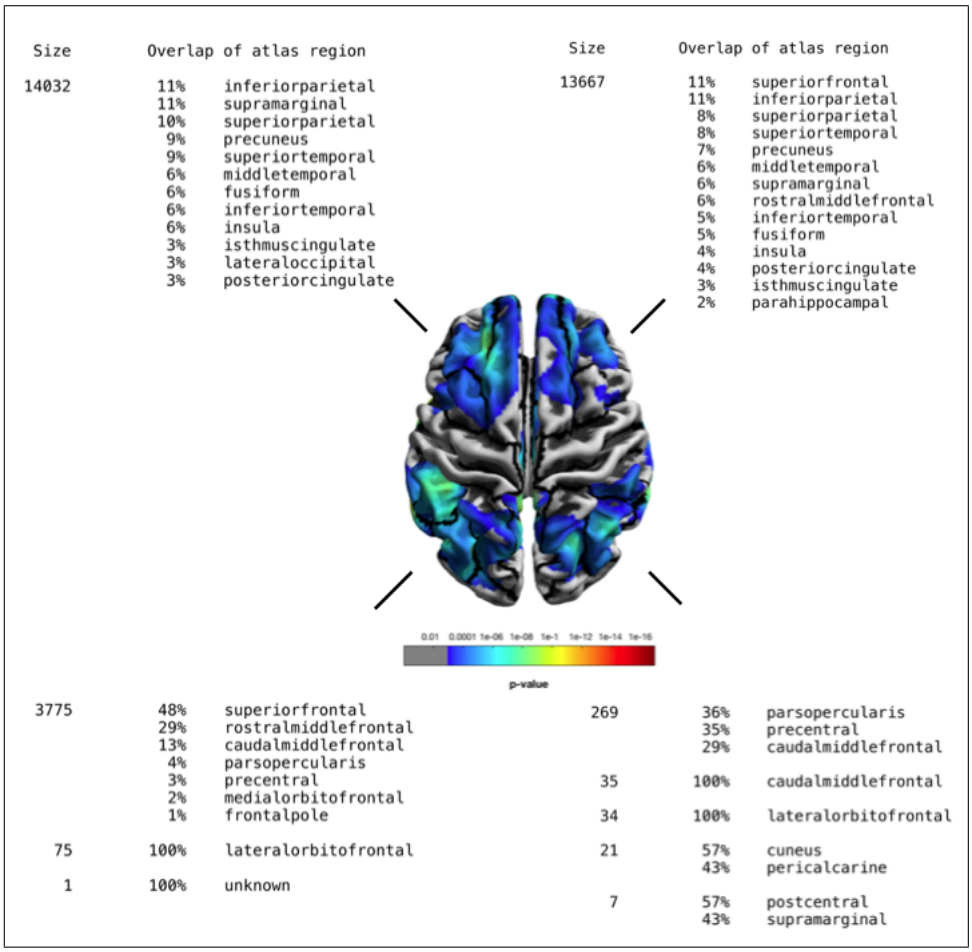

Figure 3.6 Overview of bilateral areas showing significant difference in cortical thickness between the HC and AD groups on the Desikan-Killiany atlas (FWE-corrected). Overlap of the cortical thickness change on the atlas regions are shown as percentages and the number of vertices.

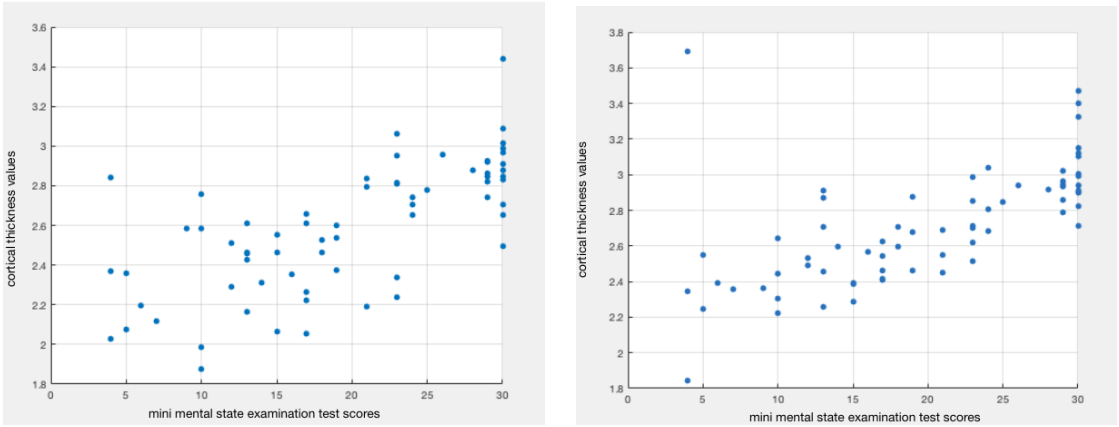

Figure 3.7 Cortical thickness values versus MMSE scores for the middle temporal region for left (left panel) and right (right panel) hemispheres. The linear correlation coefficient was estimated as 0.64 ($p<0.5$) for the right and 0.70 ($p<0.5$) for the left hemispheres.

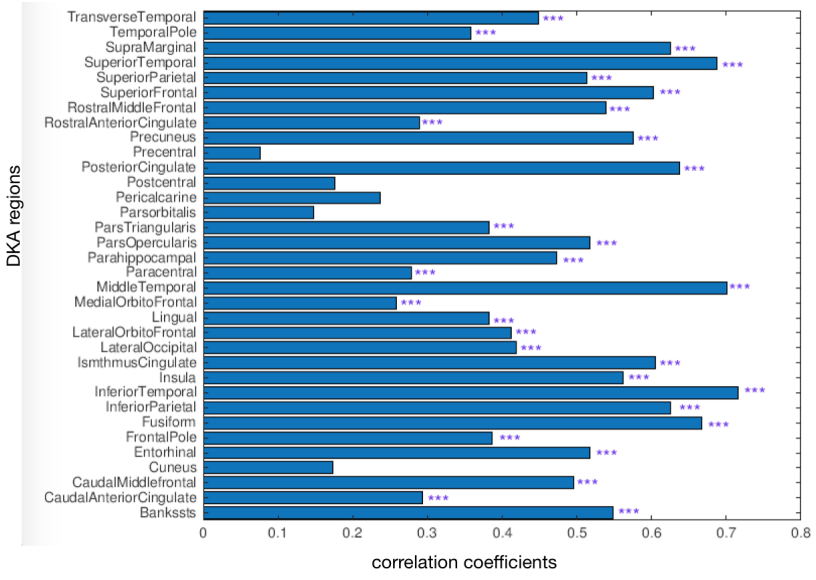

Figure 3.8 Left hemisphere correlation cofficients over 34 regions. Significance is shown as *** ($p<0.05$).

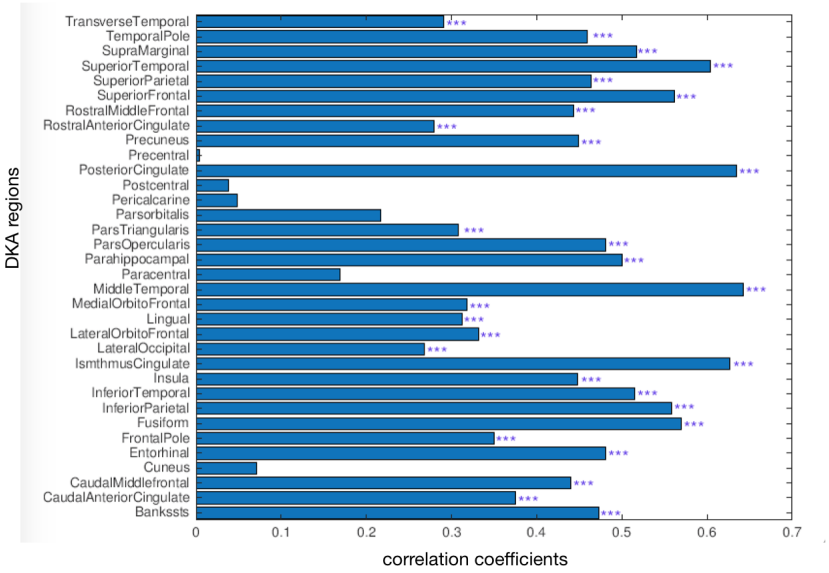

Figure 3.9 Right hemisphere correlation cofficients over 34 regions. Significance is shown as *** ($p<0.05$).

4. DISCUSSION and CONCLUSIONS

Cerebral cortical thickness was evaluated in several studies and was determined to be an important biomarker for normal neurological status, aging [27, 28] and pathological changes in brain cortical structure [29, 30]. Temporal, orbitofrontal and parietal regions of the brain are shown to be affected early and deeply during the course of the disease as reported in MRI and histological studies [31]. The most prominent changes were seen in the allocortical region of the medial temporal lobes serving as a boundary for the parahippocampal gyrus, with a reduction more than 1.25 mm in its cortical thickness [31].

In our study, an automated technique was used to evaluate the cortical thickness in the brain to study the differences in AD patients and control subjects. Also estimated were the correlations between cortical thickness and MMSE scores. The results clearly demonstrated a reduction in cortical thickness associated with AD in several areas of the brain. Most of these results have also been reported in former MRI studies [32, 28].

4.1 Discussions

Significant positive correlations were estimated for cortical thickness in certain areas such as bilateral medial parietal, supramarginal, lateral parietal and fusiform cortices, in addition to superior, middle frontal and inferior lateral temporal cortex fragments [32]. Similarly, we observed a significant cortical thickness decline in AD patients with respect to the HC group in 24 regions, both in the left and in the right hemispheres which are bankssts, caudal middle frontal, entorhinal, frontal pole, fusiform, inferior parietal, inferior temporal, insula, isthmus cingulate, lateral orbito frontal, lingual, medial orbito frontal, middle temporal, parahippocampal, pars opercularis, posterior cingulate, precuneus, rostral middle frontal, superior frontal, superior parietal, superior temporal, supra marginal, temporal pole, transverse temporal.

On the other hand, no cortical thickness change was observed in 8 regions on the left hemisphere *i.e.* caudal anterior cingulate, cuneus, paracentral, pars orbitalis, perical carine, postcentral, precentral, rostral anterior cingulate and 9 on the right *i.e.* lateral occipital, pars triangularis, cuneus, paracentral, pars orbitalis, perical carine, postcentral, precentral, rostral anterior cingulate.

Progressive atrophy was reported to effect bilaterally the anterior frontal and temporal lobes and the posterior cingulate [8] which confirms our results as given in Figure 3.3 and Figure 3.6. In addition to that, we also noticed a change in the parietal lobe.

MMSE is an important neurological test for an early diagnosis of AD which assesses the cognitive performance of the patients. It consists of several constituents as orientation, memory, attention, recall, calculation and language over a maximum scale of 30. Scores less than or equal to 25 indicate a possibility for dementia. The test is easy and fast to apply but it may yield false positives for subjects having poorer language comprehension and false negatives for those having a higher educational background. Previous studies reported a cortical volume decrease in AD patients correlating with their poorer MMSE scores [33]. Gray matter atrophy was also shown to be related with lower MMSE scores [34].

In particular, we investigated which parts of the cortical surface correlate with MMSE scores across the AD and HC groups. Statistically significant correlations between the MMSE scores and the cortical thickness in the HC and AD groups in two different regions are presented in Figure 3.7. This shows that MMSE is related to morphometric changes in the cortex associated with AD.

Our correlation results both in AD and HC groups showed that MMSE scores were related to 28 common regions on both hemispheres namely bankssts, caudal anterior cingulate, caudal middle frontal, entorhinal, frontal pole, fusiform, inferior parietal, inferior temporal, insula, isthmus cingulate, lateral occipital, lateral orbito frontal, lingual, medial orbito frontal, middle temporal, parahippocampal, pars opercularis, pars

triangularis, posterior cingulate, precuneus, rostral anterior cingulate, rostral middle frontal, superior frontal, superior parietal, superior temporal, supra marginal, temporal pole, transverse temporal (Figures 3.8 and 3.9). Except for 6 regions on the right *i.e.* precentral, paracentral, postcentral, pericalcarine, parsorbitalis, cuneus and 5 on the left *i.e.* precentral, postcentral, pericalcarine, parsorbitalis, cuneus, we observed a strong correlation between MMSE scores and all the remaining regions. The highest correlation on the right hemisphere was found to be as 0.6422 on the middle-temporal region which was believed to be related with processes as estimating distance, recognition of familiar images, and acquiring word meaning while reading. On the left hemisphere, it was the inferior temporal cortex which was assumed to be responsible for visual information processing and object recognition, that revealed a highest correlation value of 0.7163. A very similar result was reported in [35] with the highest correlation regions to be as inferior parietal and middle temporal with regard to inferior temporal and middle temporal in ours. In the case of [8], significant findings with cortical atrophy were found to be dominant on the left hemisphere whereas our results indicated a higher number of correlated regions on the right hemisphere.

4.2 Conclusions

The MMSE was known to be related with macrostructural changes in the cortex in AD [36]. Although MMSE and hippocampal volume were shown to be related, our results demonstrated that there was a significant relation between the MMSE scores and cortical atrophy associated with AD especially in large cortical and subcortical brain regions.

As mentioned above, our study showed that patients with AD showed areas of atrophy throughout the brain which was concentrated in areas related to learning, memory, language understanding, information integration and other cognitive functions. Our results also indicated that cortical thickness was reduced in the parietal, temporal, frontal, cingulate and occipital lobes as reported in previous studies.

The major advantage of the technique used in this study compared with other methods used to analyze AD is its surface based description of the actual cortex yielding a more accurate tissue quantification especially in gyral and sulcal regions. On the other hand, as a fundamental pitfall, our method restricts itself to the cortical surface therby missing the changes in subcortical structures.

4.3 Future Directions

Cortical thickness measurement may be used as a biomarker for neuronal loss associated with the temporal progress of AD. The longitudinal analysis involving multiple MRI of the same subject over a span of time can be used in AD normal populations to establish the method. Our findings may be biased due to the limited sample size which, therefore, may be replicated using a larger database [37].

The surface-based method can be extended to characterize the limiting values for the healthy and pathological groups from a certain age, sex or educational background. Normative data for specific disease groups may be used to set standards for cortical thickness. This method may help in the diagnosis of early dementia. Furthermore, cortical thickness analysis offers an extended quantification of the cerebral surface which make it also a plausible technique to establish a differential diagnosis of various sorts of dementia.

REFERENCES

1. Dahnke, R., R. Yotter, and C. Gaser, "Cortical thickness and central surface estimation" *NeuroImage*, Vol. 65, 10 2012.

2. S Desikan, R., F. Segonne, B. Fischl, B. T Quinn, B. Dickerson, D. Blacker, R. Buckner, A. Dale, R. Maguire, B. Hyman, M. S Albert, and R. J Killiany, "An automated labeling system for subdiving the human cerebral cortex on MRI scans into gyral based regions of interest" *NeuroImage*, Vol. 31, pp. 968–80, 08 2006.

3. W Small, G., E. Agdeppa, V. Kepe, N. Satyamurthy, S. and C. Huang, and J. R Barrio, "In vivo brain imaging of tangle burden in humans" *Journal of molecular neuroscience : MN*, Vol. 19, pp. 323–7, 01 2003.

4. Organization, W. H., "Dementia-rates of dementia," preprint, World Health Organization, https://www.who.int/news-room/fact-sheets/detail/dementia, 1 2017. Global action plan on the public health response to Dementia 2017 - 2025.

5. Braak H., B. E., "Neuropathological stageing of Alzheimer-related changes" *Acta Neuropathologica*, Vol. 82, pp. 239–259, Jan 1991.

6. Juottonen, K., M. Laakso, R. Insausti, M. Lehtovirta, A. Pitkanen, K. Partanen, and H. Soininen, "Volumes of the entorhinal and perirhinal cortices in Alzheimer's disease" *Neurobiology of Aging*, Vol. 19, pp. 15–22, 02 1998.

7. Mungas, D., B. Reed, W. Jagust, C. DeCarli, W. Mack, J. Kramer, M. Weiner, N. Schuff, and H. Chui, "Volumetric MRI predicts rate of cognitive decline related to AD and cerebrovascular disease" *Neurology*, Vol. 59, pp. 867–73, 10 2002.

8. P Lerch, J., J. C Pruessner, A. Zijdenbos, H. Hampel, S. Teipel, and A. Evans, "Focal decline of cortical thickness in Alzheimer's disease identified by computational neuroanatomy" *Cerebral Cortex (New York, N.Y. : 1991)*, Vol. 15, pp. 995–1001, 07 2005.

9. C. Gaser, R. D., "A computational anatomy toolbox for the analysis of structural MRI data" *HBM 2016*, Vol. 16, pp. 995–1001, 2016.

10. *BrainSuite*. Available: http://brainsuite.org/.

11. Mangin, J.-F., V. Frouin, I. Bloch, J. Regis, and J. Krahe, "From 3D magnetic resonance images to structural representations of the cortex topography using topology preserving deformations" *Journal of Mathematical Imaging and Vision*, Vol. 5, pp. 297–318, 12 1995.

12. Fischl, B., and A. Dale, "Measuring the thickness of the human cerebral cortex from magnetic resonance images" *Proceedings of the National Academy of Sciences of the United States of America*, Vol. 97, pp. 11050–5, 10 2000.

13. Zhang, K., and T. Sejnowski, "Universal scaling law between gray matter and white matter of cerebral cortex" *Proceedings of the National Academy of Sciences of the United States of America*, Vol. 97, pp. 5621–6, 06 2000.

14. Yotter, R., I. Nenadic, G. Ziegler, P. Thompson, and C. Gaser, "Local cortical surface complexity maps from spherical harmonic reconstructions" *NeuroImage*, Vol. 56, pp. 961–73, 02 2011.

15. Fischl, B., D. Salat, E. Busa, M. Albert, M. Dieterich, C. Haselgrove, A. van der Kouwe, R. Killiany, D. Kennedy, S. Klaveness, A. Montillo, N. Makris, B. Rosen, and A. Dale, "Whole brain segmentation: Automated labeling of neuroanatomical structures in the human brain" *Neuron*, Vol. 33, pp. 341–55, 02 2002.

16. Redolfi, A., D. Manset, F. Barkhof, L.-O. Wahlund, T. Glatard, J.-F. Mangin, and G. B Frisoni, "Head-to-head comparison of two popular cortical thickness extraction algorithms: A cross-sectional and longitudinal study," *PloS One*, Vol. 10, p. e0117692, 03 2015.

17. Blanc, F., S. Colloby, N. Philippi, X. de Petigny, B. Jung, C. Demuynck, C. Phillipps, P. Anthony, A. Thomas, F. Bing, J. Lamy, C. Martin-Hunyadi, J. O'Brien, B. Cretin, I. Mckeith, J. Armspach, and J.-P. Taylor, "Cortical thickness in Dementia with lewy bodies and Alzheimer's disease: A comparison of prodromal and dementia stages" *PloS One*, Vol. 10, p. e0127396, 06 2015.

18. Velayudhan, L., P. Proitsi, E. Westman, J.-S. Muehlboeck, P. Mecocci, B. Vellas, M. Tsolaki, I. Kloszewska, H. Soininen, C. Spenger, A. Hodges, J. Powell, S. Lovestone, and A. Simmons, "Entorhinal cortex thickness predicts cognitive decline in Alzheimer's disease" *Journal of Alzheimer's disease : JAD*, Vol. 33, 10 2012.

19. Du, A., N. Schuff, X. Zhu, W. Jagust, B. Miller, B. Reed, J. Kramer, D. Mungas, K. Yaffe, H. Chui, and M. Weiner, "Atrophy rates of entorhinal cortex in AD and normal aging" *Neurology*, Vol. 60, pp. 481–6, 02 2003.

20. Pennanen, C., M. Kivipelto, S. Tuomainen, P. Hartikainen, T. Hanninen, M. Laakso, M. Hallikainen, M. Vanhanen, A. Nissinen, E.-L. Helkala, P. Vainio, R. Vanninen, K. Partanen, and H. Soininen, "Hippocampus and entorhinal cortex in mild cognitive impairment and early AD" *Neurobiology of Aging*, Vol. 25, pp. 303–10, 04 2004.

21. Yotter, R., P. Thompson, and C. Gaser, "Algorithms to improve the reparameterization of spherical mappings of brain surface meshes" *Journal of Neuroimaging : Official Journal of the American Society of Neuroimaging*, Vol. 21, pp. e134–47, 04 2011.

22. Yotter, R., R. Dahnke, P. Thompson, and C. Gaser, "Topological correction of brain surface meshes using spherical harmonics" *Human Brain Mapping*, Vol. 32, pp. 1109–24, 07 2011.

23. Malone, I., D. Cash, G. Ridgway, D. Macmanus, S. Ourselin, N. C Fox, and J. M Schott, "MIRIAD-public release of a multiple time point Alzheimer's MR imaging dataset" *NeuroImage*, Vol. 70, 12 2012.

24. Potvin, O., L. Dieumegarde, and S. Duchesne, "Freesurfer cortical normative data for adults using Desikan-Killiany-Tourville and ex vivo protocols" *NeuroImage*, Vol. 156, 05 2017.

25. Handly, N., "Automated mri measures identify individuals with mild cognitive impairment and Alzheimer's disease" *Yearbook of Emergency Medicine*, Vol. 2010, pp. 96–97, 01 2010.

26. Brett, M., W. Penny, and S. Kiebel, "An introduction to random field theory" *Transactions on Rough Sets*, 01 2004.

27. M Fjell, A., K. Walhovd, I. Reinvang, A. Lundervold, D. Salat, B. T Quinn, B. Fischl, and A. Dale, "Selective increase of cortical thickness in high-performing elderly - structural indices of optimal cognitive aging" *NeuroImage*, Vol. 29, pp. 984–94, 03 2006.

28. R Sowell, E., B. Peterson, P. Thompson, S. Welcome, A. L Henkenius, and A. W Toga, "Mapping cortical change across the lifespan" *Nature Neuroscience*, Vol. 6, pp. 309–15, 04 2003.

29. Thompson, P., M. S Mega, R. P Woods, C. I Zoumalan, C. J Lindshield, R. Blanton, J. Moussai, C. Holmes, J. L Cummings, and A. Toga, "Cortical change in Alzheimer's disease detected with a disease-specific population-based brain atlas" *Cerebral cortex (New York, N.Y. : 1991)*, Vol. 11, pp. 1–16, 01 2001.

30. Rosas, H., D. Salat, S. Y Lee, A. Zaleta, V. Pappu, B. Fischl, D. Greve, N. Hevelone, and S. Hersch, "Cerebral cortex and the clinical expression of Huntington's disease: Complexity and heterogeneity" *Brain : A Journal of Neurology*, Vol. 131, pp. 1057–68, 05 2008.

31. de Leon, M., M. Bobinski, A. Convit, O. Wolf, and R. Insausti, "Usefulness of mri measures of entorhinal cortex versus hippocampus in AD" *Neurology*, Vol. 56, pp. 820–1, 04 2001.

32. Yang, H., H. Xu, Q. Li, Y. Jin, W. Jiang, J. Wang, Y. Wu, W. Li, C. Yang, X. Li, S. Xiao, F. Shi, and T. Wang, "Study of brain morphology change in Alzheimer's disease and amnestic mild cognitive impairment compared with normal controls" *General Psychiatry*, Vol. 32, p. e100005, 04 2019.

33. Mouton, P. R., L. J. Martin, M. E. Calhoun, G. Dal Forno, and D. L. Price, "Cognitive decline strongly correlates with cortical atrophy in Alzheimer's dementia" *Neurobiol Aging*, Vol. 19, pp. 371–377, 09 1998.

34. Baxter, L., D. Sparks, S. C Johnson, B. Lenoski, J. E Lopez, D. J Connor, and M. Sabbagh, "Relationship of cognitive measures and gray and white matter in Alzheimer's disease" *Journal of Alzheimer's disease : JAD*, Vol. 9, pp. 253–60, 09 2006.

35. M Fjell, A., K. Walhovd, C. Fennema-Notestine, L. Mcevoy, D. Hagler, D. Holland, J. B Brewer, and A. Dale, "One-year brain atrophy evident in healthy aging," *The Journal of Neuroscience : The Official Journal of the Society for Neuroscience*, Vol. 29, pp. 15223–31, 12 2009.

36. Yavuz, B., S. Ariogul, M. Cankurtaran, K. Oguz, M. Halil, N. Dagli, and E. Sahin Cankurtaran, "Hippocampal atrophy correlates with the severity of cognitive decline" *International psychogeriatrics / IPA*, Vol. 19, pp. 767–77, 09 2007.

37. Cronin-Golomb, A., S. Corkin, J. F. Rizzo, J. Cohen, J. H. Growdon, and K. S. Banks, "Visual dysfunction in Alzheimer disease: Relation to normal aging" *Annals of Neurology*, Vol. 29, pp. 41–52, 01 1991.